

Development, Validation, and Application of a Parametric Pediatric Head Finite Element Model for Impact Simulations

ZHIGANG LI,^{1,2} JINGWEN HU,¹ MATTHEW P. REED,¹ JONATHAN D. RUPP,¹ CARRIE N. HOFF,³
JINHUAN ZHANG,² and BO CHENG²

¹University of Michigan Transportation Research Institute, Ann Arbor, MI, USA; ²State Key Laboratory of Automotive Safety and Energy, Tsinghua University, Beijing, China; and ³Department of Radiology, University of Michigan, Ann Arbor, MI, USA

(Received 27 May 2011; accepted 15 September 2011; published online 24 September 2011)

Associate Editor Eiji Tanaka oversaw the review of this article.

Abstract—In this study, a statistical model of cranium geometry for 0- to 3-month-old children was developed by analyzing 11 CT scans using a combination of principal component analysis and multivariate regression analysis. Radial basis function was used to morph the geometry of a baseline child head finite element (FE) model into models with geometries representing a newborn, a 1.5-month-old, and a 3-month-old infant head. These three FE models were used in a parametric study of near-vertex impact conditions to quantify the sensitivity of different material parameters. Finally, model validation was conducted against peak head accelerations in cadaver tests under different impact conditions, and optimization techniques were used to determine the material properties. The results showed that the statistical model of cranium geometry produced realistic cranium size and shape, suture size, and skull/suture thickness, for 0- to 3-month-old children. The three pediatric head models generated by morphing had mesh quality comparable to the baseline model. The elastic modulus of skull had a greater effect on most head impact response measurements than other parameters. Head geometry was a significant factor affecting the maximal principal stress of the skull ($p = 0.002$) and maximal principal strain of the suture ($p = 0.021$) after controlling for the skull material. Compared with the newborn head, the 3-month-old head model produced 6.5% higher peak head acceleration, 64.8% higher maximal principal stress, and 66.3% higher strain in the suture. However, in the skull, the 3-month-old model produced 25.7% lower maximal principal stress and 11.5% lower strain than the newborn head. Material properties of the brain had little effects on head acceleration and strain/stress within the skull and suture. Elastic moduli of the skull, suture, dura, and scalp determined using optimization techniques were within reported literature ranges and produced impact response that closely matched those measured in previous cadaver tests. The method developed in this study made it possible to investigate the age effects from geometry changes

on pediatric head impact responses. The parametric study demonstrated that it is important to consider the material properties and geometric variations together when estimating pediatric head responses and predicting head injury risks.

Keywords—Pediatric head injury, Parametric finite element model, Principal component analysis, Mesh morphing, Radial basis function, Parametric study, Optimization.

INTRODUCTION

Head injury is the leading cause of pediatric fatality and disability in the United States.^{1,2,15,34} The most frequent causes of pediatric head injuries are motor-vehicle crashes, falls, and maltreatment.^{7,16} Basic injury biomechanics research and injury assessment tools are essential for understanding the impact response, injury mechanisms, and the injury tolerance of the pediatric head and for providing guidelines to clinicians and design engineers for future injury diagnosis and prevention. Although the finite element (FE) method has been widely used for investigating adult head injury from impact, only a few 3D pediatric head FE models have been reported. Lapeer and Prager¹⁷ developed an infant head FE model to simulate skull deformation during the birthing process. Klinich *et al.*¹⁴ built a 6-month-old head FE model and reconstructed three motor-vehicle crashes where infants were injured due to airbag deployment. Coats *et al.*⁹ constructed a 1.5-month-old infant head FE model and conducted a parametric study to investigate the relative importance of brain material and anatomical variations in suture and scalp on head responses during short falls. Roth *et al.*^{25,27} developed a 6-month-old child head model to simulate injuries

Address correspondence to Jingwen Hu, University of Michigan Transportation Research Institute, Ann Arbor, MI, USA. Electronic mail: jwhu@umich.edu

due to shaking and fall accidents. The same group also developed a 3-year-old child head model to reconstruct 25 fall accidents^{26,29} and a 17-day-old child head model to reconstruct a child fall accident.²⁸ Details of each aforementioned model are shown in Table A1 in Appendix.

Each of these previously developed models represents a specific age and single head geometry, and therefore cannot account for variation in head morphological differences among children. To quantify the effects of head morphology on impact response and injury risk, a pediatric head FE model that has geometry that can be rapidly and appropriately varied with age is necessary. Due to the limitation of child cadavers available for testing, such a model will be extremely useful for investigating the morphology and age effects on pediatric head injuries, and thus providing insights on how to prevent those injuries.

The objectives of this study were (1) to develop a statistical geometry model describing pediatric cranium size and shape, suture size, skull/suture thickness for 0- to 3-month-old children and a parametric head FE model capable of simulating head impact responses for children with different head geometries; (2) to conduct a parametric study on the effects of both geometry and material properties on pediatric head impact response, obtaining the sensitive parameters of material properties; and (3) to use optimization techniques to calibrate the sensitive parameters of material properties of the head that best match pediatric head cadaver drop tests.

MODEL DEVELOPMENT

Model Development Procedure

As shown in Fig. 1, the approach used to develop a parametric pediatric head FE model involves

morphing a baseline model into different head geometries using mesh morphing techniques. The statistical child head geometry model was built using a sequence of procedures involving CT sampling, segmentation, landmark identification, skull/suture thickness measurement, principal component analysis (PCA), and multivariate regression analysis. Landmarks were also identified on a baseline child head FE model at the locations corresponding to those in the geometry model. During the mesh morphing procedure, shape and size of the head, and the skull/suture thickness are morphed according to landmark locations and the skull/suture thicknesses at those locations. Radial basis function (RBF), a spatial interpolation method, was used to perform mesh morphing. This set of algorithm can be applied programmatically, making them an efficient tool for generating a group of FE head models for children with different ages and head geometries. Once the FE mesh was generated, different material properties also need to be assigned to different head components based on the parametric study and material property calibration results suitable for the specific age of the child.

Baseline Model Development

The baseline model used in this study was a modified version of the 6-month-old head FE model developed by Klinich *et al.*¹⁴ Modifications to the Klinich *et al.* model included improvements in mesh quality through remeshing with only hexahedral solid elements and quadrilateral shell/membrane elements using TrueGrid 2.3.4 (XYZ Scientific Application, Inc, California). The minimal Jacobian of the solid elements in the new mesh was greater than 0.4. Note that the Jacobian ratio is a measurement of the deviation of a given element from an ideally shaped element. The Jacobian value ranges from -1.0 to 1.0 , where

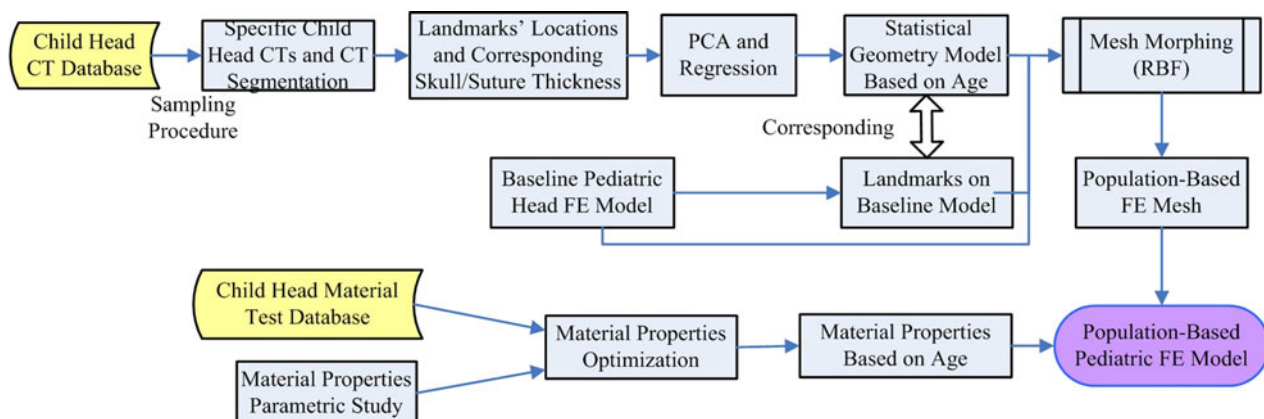


FIGURE 1. Flowchart of the procedure to develop a pediatric parametric head FE model.

1.0 represents a perfectly shaped element. In the current study, we evaluated the determinant of the Jacobian matrix at each of the element's integration points (Gauss points) by Hypermesh software. If the local stretching is the same at all of its Gauss points, then the Jacobian value equals 1.0. As the element becomes more distorted, the Jacobian value approaches zero. Generally speaking, a minimal Jacobian value greater than 0.3 represented good mesh quality of hexahedral elements. The current model included skull, suture, brain, dura mater, cerebrospinal fluid (CSF), and scalp as shown in Fig. 2. Brain structures, such as cerebrum, cerebellum, and brain stem were not differentiated in the current model due to two reasons. First, the present study was focusing on the head overall stiffness and skull/suture responses, in which brain structure differences play little effects. Second, the material property differences among different brain structures were not well-documented and to date all the available pediatric head FE models used same material for the whole brain.

Statistical Head Geometry Model for 0- to 3-Month-Old Children

Image Processing and Landmark Identification

Head CT images from 11 subjects from 0 to 3 months without head trauma or skull abnormalities were obtained from the University of Michigan, Department of Radiology through a protocol approved by an institutional review board at the University of Michigan. A discovery CT750 HD made by GE medical system was used to carry out the scan work. All CT image sets had 2.5 mm slice spacing with resolution of 512×512 . The display field of view is 150 mm, resulting in a pixel size of 0.3 mm. Image

processing was performed using OsiriX 3.5.1 (Pixmeo, Switzerland) and involved: (1) CT images segmentation, which was conducted in 3D volume rendering mode using a Hounsfield Unit threshold value of 304 to generate skull and suture geometry, (2) landmark identification, and (3) thickness measurement at each landmark location. There are two types of landmarks defined in this study: landmarks along the suture and landmarks evenly distributed on the skull surface, as shown in Fig. 3. Because most of the landmarks along the sutures are related to anatomical features, they can be easily identified with relatively high accuracy by a person who is familiar with the head anatomical structures. However, landmarks on the skull surface generally are not associated with any anatomical features. To ensure the accuracy and consistency of landmark locations on the skull surface, landmarks on different subjects were all based on the landmark relative positions on the baseline FE model. For example, as shown in the Fig. 3, landmark No. 65 on the skull was identified in the middle between landmark No. 23 on the cortical suture and landmark No. 49 on the lambdoid suture. Landmark No. 90 was further selected in the middle between landmark No. 49 and landmark No. 65. The distances between different landmarks and the distance ratio can be easily measured and calculated for the CT images, which ensure the accuracy and consistency of the landmark identification. The number of landmarks was determined by several iterative trials. It was found that 92 landmarks on half of the head resulted in relatively accurate shape and size of the suture and skull. The head was treated as symmetrical based on previous studies,^{14,38} so landmarks were only located at half of the head in the baseline model as well as CT segmentation data. The thickness values of the skull/suture were directly measured in the skull/suture segmentation data in a direction perpendicular to the tangent plane of the skull/suture surface at the landmark locations.

The baseline FE model, CT segmentation results for the skulls and corresponding landmarks on both the FE model and CT segmentation data are shown in Fig. 3. The morphology of the heads from different subjects varied largely. Generally, the width of the fontanel and suture decreased as age increased.

PCA and Regression Analysis

PCA is a statistical technique used for data compression and organization in many research fields, such as facial feature recognition, ergonomics, and crash dummy design.^{5,22,23} When many data dimensions in original data set are correlated, the first few principal components (PCs) can include most variance of the whole data set, so the data dimensions with low

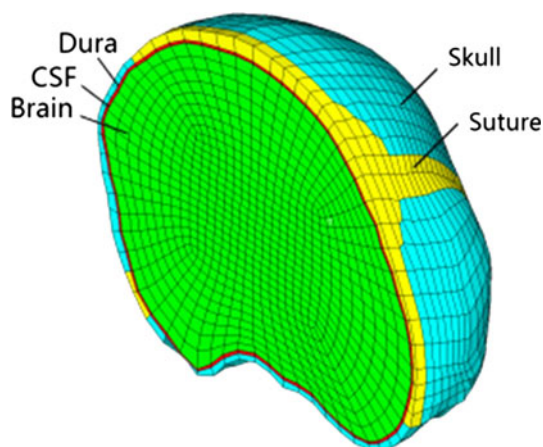


FIGURE 2. Components in half of the baseline model.

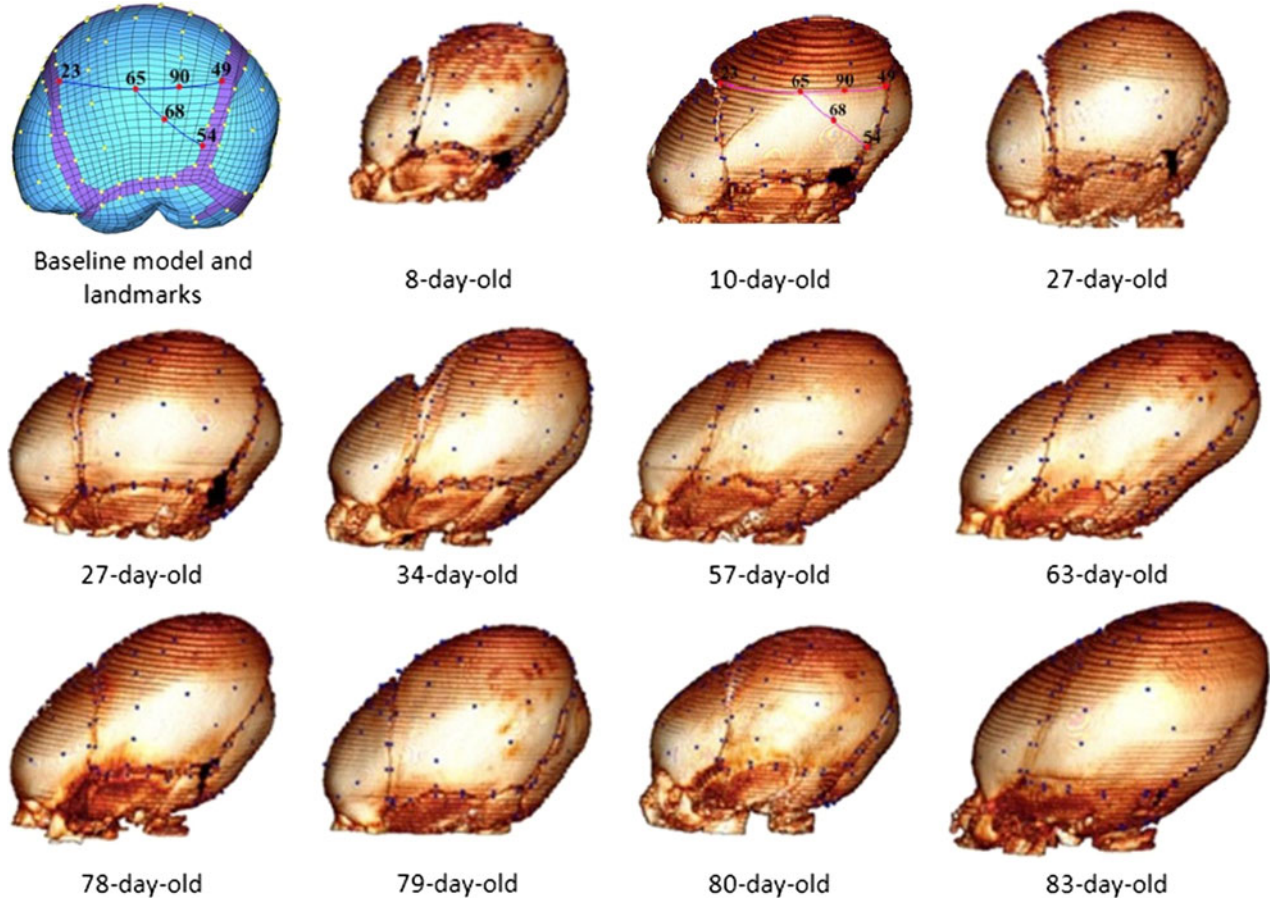


FIGURE 3. Landmarks, baseline FE model, and CT segmentation.

variance can be eliminated with minimal loss of information. The first PC represents the direction with the highest variance in the data and the second PC represents the second highest variance with a direction orthogonal to the first PC, and so on.

In the current study, there are 11 (N) subjects and each with 92 landmarks. Three coordinates and one skull thickness at each of these landmarks formed a head geometry vector with a length of $l = 92 \times 4 = 368$ denoted as \mathbf{g} . The geometry vector for each child head was joined together to construct an 11×368 geometry matrix \mathbf{G}_1 . In order to make PCA method work properly, the geometry matrix \mathbf{G}_1 needed to subtract the mean $\bar{\mathbf{g}}$ from each of the individual's \mathbf{g}_i which called data centered matrix \mathbf{G} . PCA can be computed through calculating the eigenvalues and eigenvectors of covariance matrix of centered geometry \mathbf{G} . According to studies by Turk and Pentland³³ and Reed *et al.*,²² \mathbf{G} can be decomposed as follows,

$$\mathbf{G} = \mathbf{S}\mathbf{P}$$

$$\mathbf{S} = \mathbf{G}\mathbf{P}^T$$

where \mathbf{S} is an $N \times l$ matrix called PC scores and \mathbf{P} is the eigenvectors of \mathbf{G} , which is an $l \times l$ normalized matrix.

The matrix \mathbf{G} can be closely approximated (cumulative variance $>90\%$) by taking the first k PCs,

$$\mathbf{G}^* = \mathbf{S}_k\mathbf{P}_k$$

where \mathbf{G}^* is the approximation of \mathbf{G} , \mathbf{S}_k is the first k column of \mathbf{S} , and \mathbf{P}_k is the first k rows of \mathbf{P} .

Any individual's coordinates and skull thickness of landmarks can be obtained based on the equation as

$$\mathbf{g}_i^* = \bar{\mathbf{g}} + \mathbf{P}_N^T \mathbf{S}_{Ni}^T$$

where \mathbf{S}_{Ni} is the row of matrix \mathbf{S}_N corresponding to the i th individual's PC scores.

In order to use parameters, such as age and head circumference, to predict PC scores (\mathbf{S}_k), in turn, to predict detailed head geometry, a regression model was generated following the procedure in Reed *et al.*²² as follows,

$$\mathbf{S}_k^T = \mathbf{C}\mathbf{F} + \boldsymbol{\varepsilon}^T$$

where F is the feature matrix, C is the coefficient matrix, ε^T is a vector of zero mean and normally distributed residuals. Ignoring ε^T , C can be obtained using the standard least-squares techniques by taking the Moore–Penrose pseudo-inverse of F , given

$$C = S_k^T F^{-1}$$

where F^{-1} is the Moore–Penrose pseudo-inverse of F .

As expected, the coordinates and thicknesses of the landmarks were accurately represented by a small number of PCs. For the coordinates, over 99% variance was represented by the first 9 PCs, while for the thickness information, more than 96% variance was described by the first 9 PCs. As a result, in this study, 9 PCs were used for the following regression analysis. For children from 0- to 3-month-old, head growth results in significant morphology changes over short periods of time. Therefore, in this study, age was considered as the only input parameter in the regression model to predict the head geometry. Landmark locations for children at age of 0, 1.5, and 3 months were generated using PCA and regression analysis as shown in Fig. 4.

Parametric Child Head FE Model

RBF Interpolation

RBF interpolation is widely used in diverse fields, including image processing, meteorology, and medical MRI data operation. The basic concepts and formulas of the RBF have been provided in many

references^{3,6,13,19} In the present study, the thin-plate spline function $\varphi = r^2 \log(r)$ was selected as the most suitable basic function for mesh morphing in terms of geometry accuracy and mesh quality.

Mesh Morphing

In the morphing process, the baseline model was morphed to the target child head geometry, and skull/suture thickness distribution was adjusted to match the target thickness based on the geometry model.

The morphing results from the baseline model into child head models at three ages are shown in Fig. 5. There are 38,912 solid elements and 7,680 shell elements in each model. The mesh qualities for all three models were close to the baseline model. The minimum Jacobian of the baseline model is 0.4, while for newborn, 1.5-month-old, 3-month-old, the number of elements with Jacobian less than 0.4 were only 22, 20, and 28, respectively. The thickness of the scalp was assumed to be constant throughout the head.

To evaluate the accuracy of the geometry after mesh morphing, subject-specific head FE models for all 11 subjects were generated by the morphing method. Ten non-landmark locations along the suture were selected on both the morphed models and CT images, and the location errors were calculated for each subject. The maximal error of these ten locations on the 11 subjects was 1.5 mm.

Material Properties

An extensive literature review on child head material properties by Franklyn *et al.*¹² has compared and summarized most of the previous experimental data available before 2006. Coats *et al.*⁸ conducted bending and tension tests on skull and suture using 23 pediatric cadavers from 21 weeks gestational age to 13-month old. The results showed that age and location did not have significant effects on elastic modulus of skulls from 0- to 13-month-old children. Therefore, in this study, the skull was assumed homogeneous and the same elastic modulus was used in 0- to 3-month-old head models.

The material properties of skull, suture, dura, and scalp were considered as linear elastic and were determined through optimization techniques (see Table 2), which was described in the next two sections. The material properties of the CSF were taken from Willinger *et al.*³⁷ Brain was considered as linear viscoelastic and parameter values were from Roth *et al.*²⁸ and Thibault *et al.*³² Because the three head models constructed in this study have a narrow age scope, only one set of material properties of pediatric head components (see Table 2) was applied to these three models.

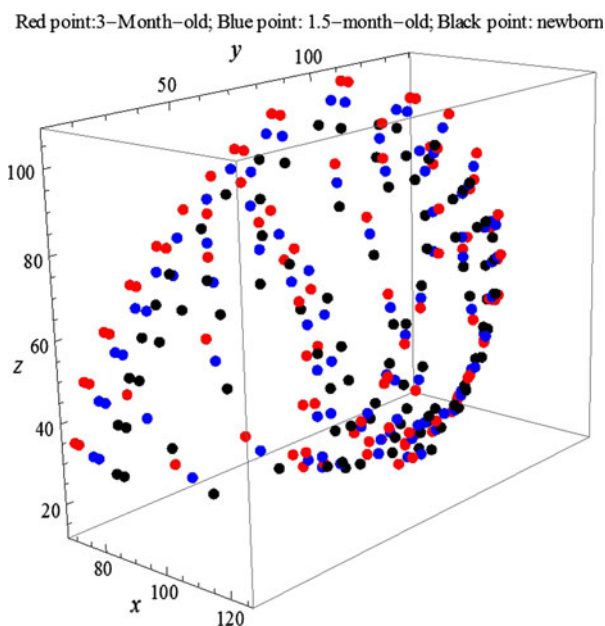


FIGURE 4. Predicted landmark spatial locations for half of the pediatric heads at three ages (unit: mm).

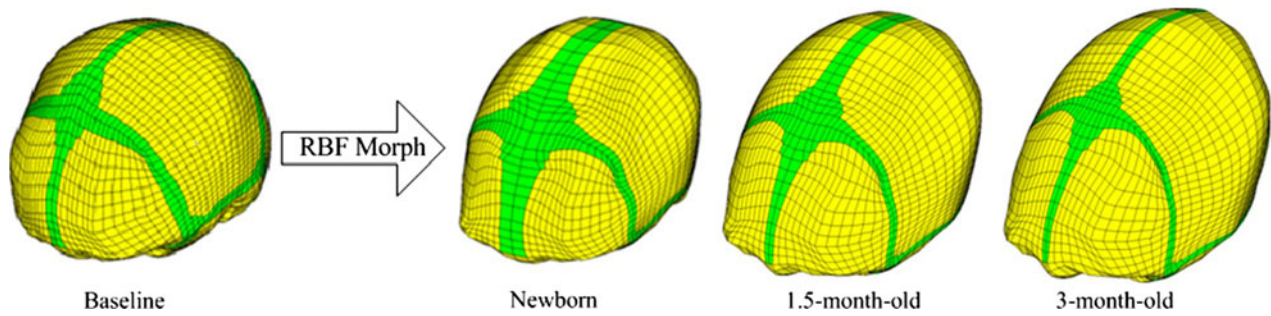


FIGURE 5. Morphing results from baseline model to three targets.

TABLE 1. Levels of factors selected for the computational experiment.

Level	Skull_E (MPa)	Suture_E (MPa)	Dura_E (MPa)	Scalp_E (MPa)	G_0/G_∞ (MPa)	β (1/s)	Age (days)
1	29	4	16	8.5	0.006/0.00232	35	8
2	673.5	10	40	21.25	0.0275/0.01065	477.5	45
3	1318	16	64	34	0.049/0.01898	920	90

Note: G_0 and G_∞ change correspondingly, thus was deemed as one factor.

PARAMETRIC STUDY ON MATERIAL PROPERTIES AND HEAD MORPHOLOGY

Only a few experimental studies are available in the literature for pediatric head material properties and there are large discrepancies among them. Several parametric studies have been conducted by Klinich *et al.*,¹⁴ Coats *et al.*,⁹ and Roth *et al.*²⁸ to investigate the material effects on pediatric head impact responses. However, all of them were only based on a single FE head model, which cannot account for the geometry changes due to child growth. The parametric model developed in this study provided a tool to investigate the effects from material property and geometry at the same time.

In this study, a computational experiment was performed under the condition of dropping the FE model from 30 cm height onto a rigid surface and impact with the vertex as shown in Fig. 7. The initial velocity of the head model was calculated based on the drop height. A surface-to-surface contact was used to define the contact between the head and the rigid surface in all the simulations. The friction coefficient was set at 0.2 between the head and the impact surface. In order to reduce simulation times, the Taguchi method was used to determine the simulation number and parameter combinations. A total of eight factors were considered in the Taguchi array, including elastic modulus of the skull (Skull_E), suture (Suture_E), dura (Dura_E), and scalp (Scalp_E), short-term shear modulus (G_0), long-term shear modulus (G_∞), and decay coefficient (β) of the brain, and age. Note that age is a factor only representing the morphology changes during child growth but not the material property change. In the

Taguchi array, three levels were selected for each factor (see Table 1), resulting in 27 simulations. The selected range of elastic modulus of skull was based on the study by Coats *et al.*⁸ The ranges of elastic moduli of suture, dura, and scalp were set at 50 to 200% of baseline values, which were adopted from a 17-day-old FE model by Roth *et al.*²⁸ For the material properties of brain, the ranges of G_0 , G_∞ , and β were determined according to Roth *et al.*²⁸ In this study, G_∞ was set as 38.7% of G_0 according to the ratio reported by Roth *et al.*²⁸ The head peak acceleration, maximum principal strain, and stress within the skull and suture were selected as the injury predictors to evaluate the child head response.

To test the statistical significance of each factor, one-way analysis of variance (ANOVA) and analysis of covariance (ANCOVA) were performed using SPSS 17.0 (SPSS Inc. Chicago, IL). Model predicted injury measurements with respect to the levels of seven factors used in the Taguchi array are shown in Fig. 6. Standard errors are shown by the vertical brackets at the top of each bar, and significant levels of each factor from one-way ANOVA are indicated by the p values.

Varying elastic modulus of the skull resulted in significant differences in all response measurements. Increasing elastic modulus of the skull significantly increased head peak acceleration ($p = 0.000$), maximal principal stress of skull ($p = 0.000$) and suture ($p = 0.017$), and maximal principal strain of suture ($p = 0.003$), and could significantly decrease the maximal principal strain of skull ($p = 0.000$). Increasing elastic modulus of scalp could significantly decrease the maximal principal stress ($p = 0.004$) and strain

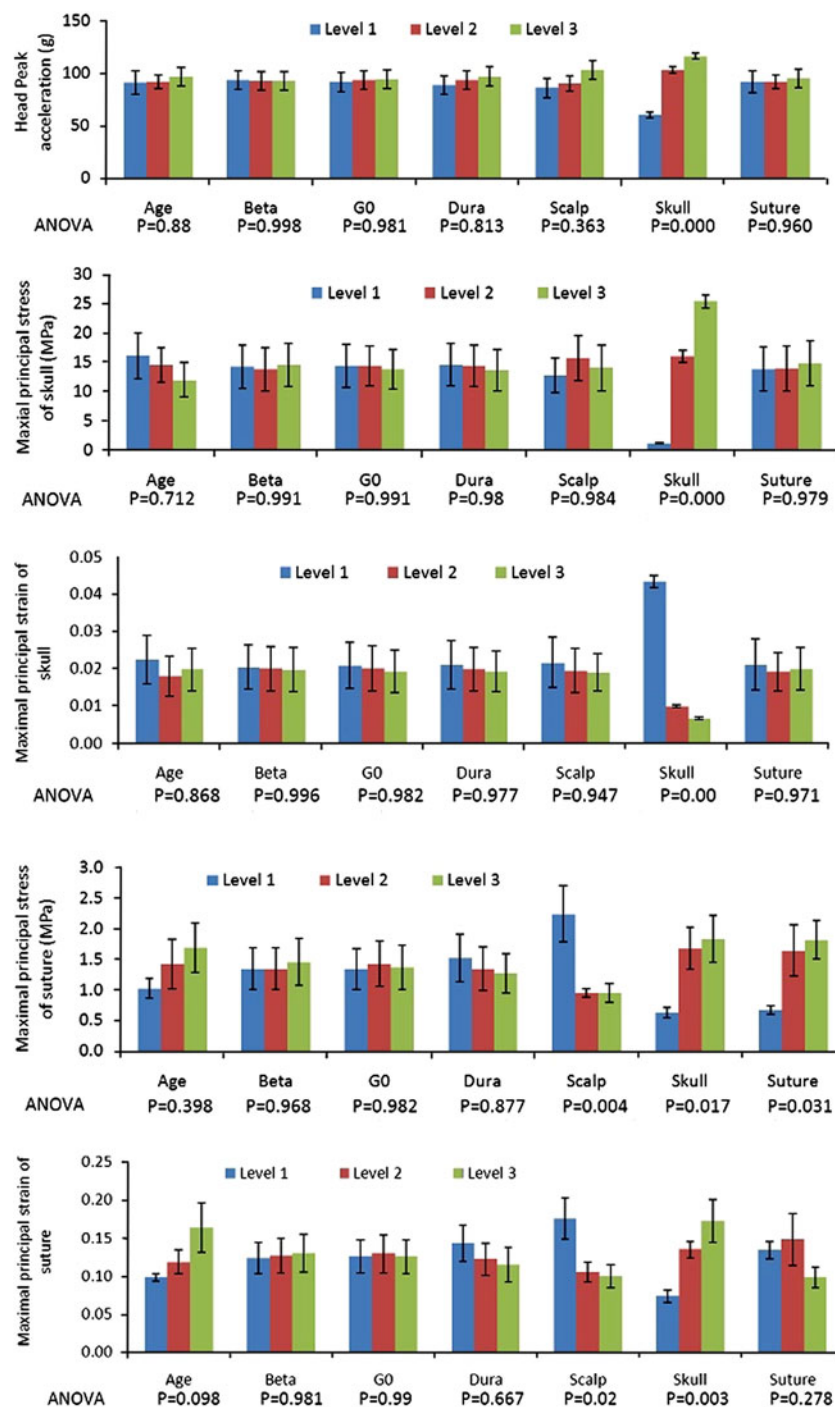


FIGURE 6. Response measurements with respect to all factors.

($p = 0.02$) of suture. Elastic modulus of the suture had a significant effect ($p = 0.031$) on maximal principal stress of the suture, and head geometry, represented by age in the simulation matrix, had a marginally significant effect ($p = 0.098$) on the strain of suture.

To determine if the factors other than skull modulus were statistically significant, a one-way ANCOVA was conducted for the remaining six factors with the elastic

modulus of skull as the covariate. After controlling the elastic modulus of skull, age was a significant factor affecting the maximal stress of skull ($p = 0.002$) and maximal strain of suture ($p = 0.021$). Scalp elastic modulus also became a significant factor affecting the head peak acceleration ($p = 0.002$), and a marginally significant factor affecting maximal stress of the skull ($p = 0.062$).

Although the child age was constrained in a small range of 0–3 months, the variations of morphology have shown fairly obvious influence on head response measurements. The three child head FE models were assigned the same material properties in the DOE, different material properties might increase the influence even more. Compared to newborn head, in average, the 3-month-old head predicted higher peak head acceleration (6.5% higher), maximal principal stress (64.8% higher), and strain (66.3% higher) of suture, but lower maximal principal stress (25.7% lower) and strain (11.5% lower) of skull.

MATERIAL PARAMETER OPTIMIZATION AND MODEL VALIDATION

Cadaver Tests of Pediatric Head

Material parameter optimization and model validation were performed by simulating tests of head from cadavers at age of 1-, 3-, and 11-day old conducted by Prange *et al.*²⁰ In these tests, pediatric heads were subjected to two different loading conditions, drop and compression. In drop tests, infant heads were dropped onto a flat smooth anvil plate under five different directions (vertex, occipital, forehead, left, and right parietal) at 15 and 30 cm heights. Mandibles were removed from the specimens during the tests. In this study, test results under left and right parietal conditions were combined because the pediatric head FE model was assumed as symmetric, so in total, four drop directions and each with two drop heights are shown in Fig. 7. In the compression tests, the infant head was placed between two parallel rigid plates. One plate is fixed and the other is moved along the anterior–posterior (AP) and right–left (RL) direction at the velocity of 0.05, 1, 10, and 50 mm/s. Because only force-deformation time history in AP direction was reported, simulations in the AP direction were conducted at 50 mm/s. The posterior of the head was fixed

to be equivalent to the test condition, as shown in Fig. 8.

Material Parameter Optimization

An inverse FE method was used to determine the material parameters by comparing the simulation results with dropping test data. In this study, the newborn pediatric head model was selected to match the dropping test results through optimization, because it is similar to the age of specimens in the test. The boundary conditions of the model were defined as same as the test conditions. The initial velocity of the head model was calculated based on the height of the drop test. A surface-to-surface contact was used to define the contact between the head and the rigid surface in the simulation. The friction coefficient was set at 0.2 in all simulations. LS-DYNA, an explicit FE software package suitable for high-speed, large deformation impact analysis, was used in this study.

The SIMPLEX optimization method was used for optimization, which uses the well-known Nelder and Mead Downhill method¹⁸ commonly used for multi-dimensional minimization problems. Figure 9 outlines how the material parameters of the pediatric head were optimized.

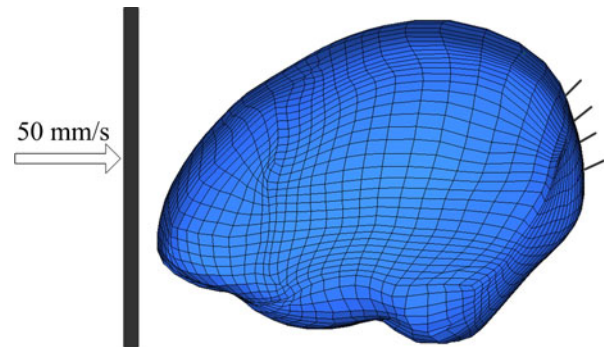


FIGURE 8. Compression test setup with moving plate at the anterior boundary and the posterior skull fixed.

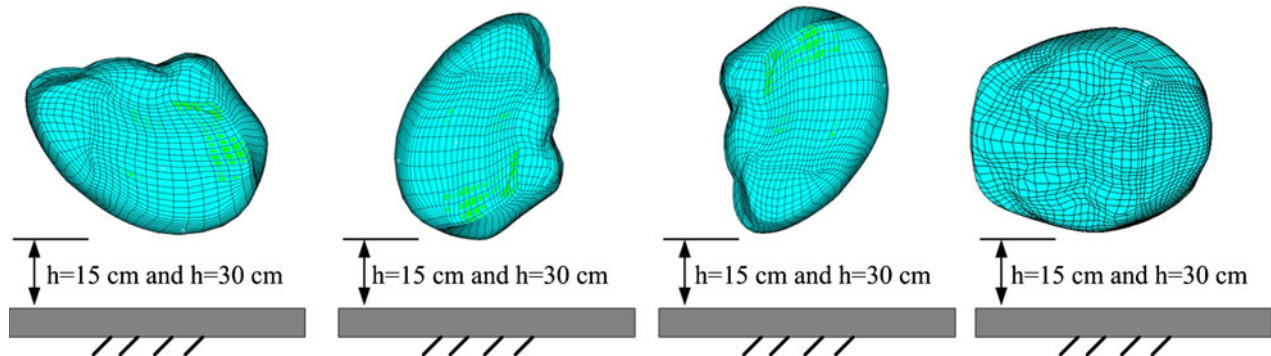


FIGURE 7. Drop test conditions.

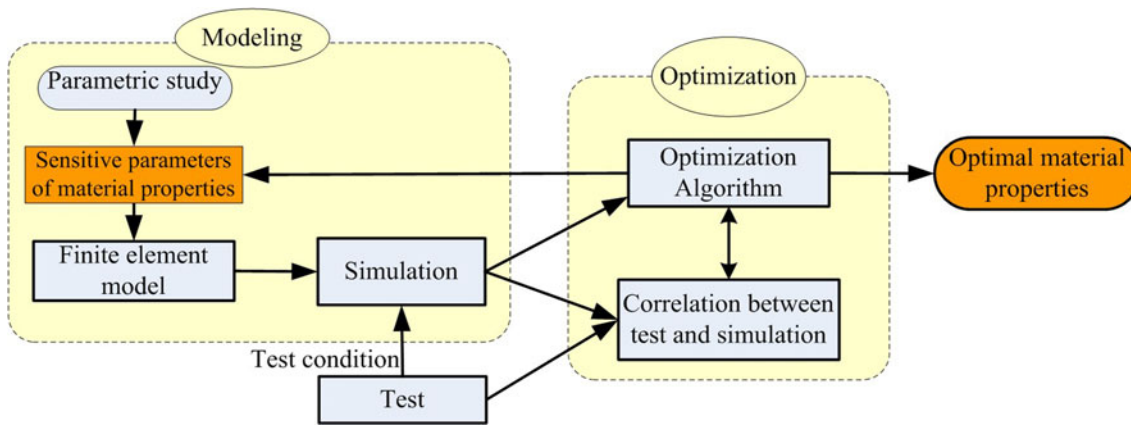


FIGURE 9. Flowchart for material parameter optimization.

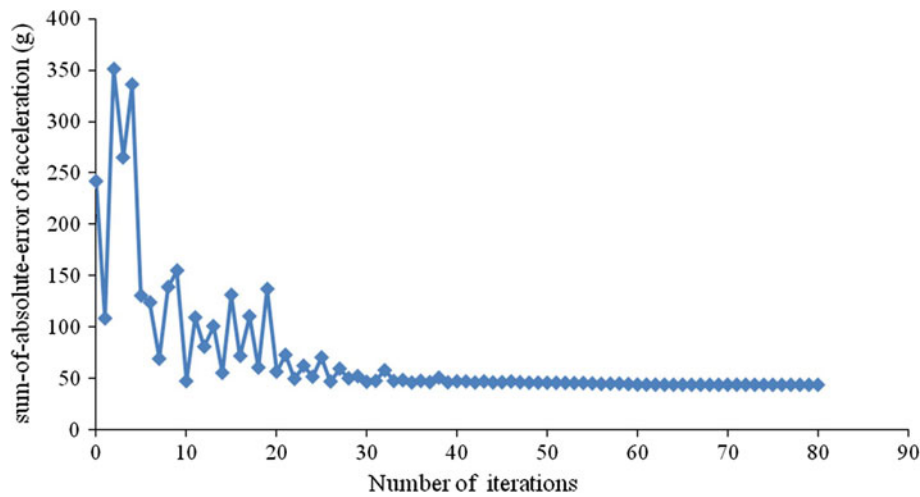


FIGURE 10. History of sum of acceleration errors in eight drop conditions in the optimization.

According to the results of the parametric study, the material parameters of the brain (G_0 , G_1 , G_∞ , and β) have little effects on the head response measurements, so only four parameters (Skull_E, Suture_E, Dura_E, Scalp_E) were used as input variables for optimization. The searching ranges of these four input variables in the optimization were the same as those in the parametric study. The sum-of-absolute-error (Eq. 1) of the peak head acceleration between the tests and simulations in eight drop conditions was considered as the objective function shown in Eq. (1). The optimization was performed using modeFRONTIER 4.3.0 (ESTECO).

$$\text{Acc}_{\text{error}} = \sum_{i=1}^8 |\text{Acc}(\text{sim}_i) - \text{Acc}(\text{Test}_i)| \quad (1)$$

where $\text{Acc}(\text{sim}_i)$ and $\text{Acc}(\text{Test}_i)$ represent the simulated and experimentally measured head peak acceleration under each drop condition.

Figure 10 shows the objective function history, in which convergence was achieved after about 40 iterations.

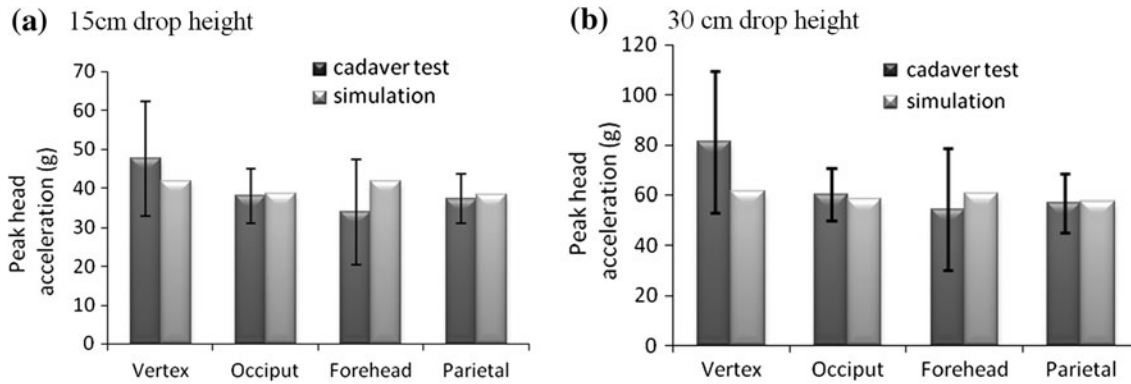
The bold values in Table 2 are the optimal results of elastic moduli of skull, suture, dura, and scalp. Simulations were conducted according to the dropping and compression cadaver test condition after putting the material properties in Table 2 into the newborn FE model. Head accelerations were compared between the tests and simulations in eight impact conditions as shown in Fig. 11. Good correlations in both 15 and 30 cm drop conditions were achieved for all impact directions except for vertex drop at 30 cm height, in which simulation result was clearly lower than the test, but still within the test corridor.

Model Validation

To further validate the model, a simulation under the compression condition described in Fig. 8 was also

TABLE 2. Material properties used in the infant head FE models.

Parameters	Young's modulus (MPa)	Poisson's ratio	Density (kg/m ³)	Note
Skull	170.79	0.22	2150	Optimization determined
Suture	8.00	0.49	1130	
Dura	21.28	0.45	1140	
Scalp	8.56	0.42	1200	
CSF	0.012	0.499	1040	From literature
Brain	$K = 2.11 \text{ GPa}$, $G(t) = G_{\infty} + (G_0 - G_{\infty})e^{-\beta t}$ $G_0 = 5.99 \text{ kPa}$, $G_{\infty} = 2.32 \text{ kPa}$, $\beta = 35/s$		1040	

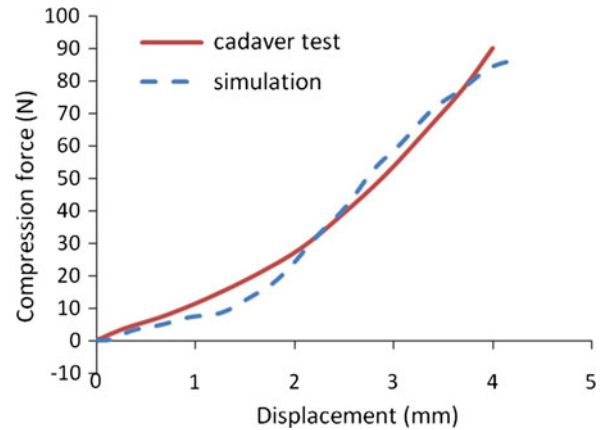
**FIGURE 11. Optimization results under different drop conditions.²⁰**

conducted using the optimal material parameters achieved in the optimization. A good correlation was also found between the test and simulation results as shown in Fig. 12, showing that the final material parameters selected for the model can provide good biofidelity of the pediatric head model in conditions other than those used in the material parameter optimization.

DISCUSSION

Statistical Pediatric Head Geometry Model and Parametric Head FE Model

Several previous studies have presented data on skull diameter, volume, and dimension with age for pediatric populations.^{11,24,31} However, due to technology limitations, only basic external dimensions were measured in those studies, and the data do not represent the detailed 3D geometry of the head. More recently, Danelson *et al.*¹⁰ used MR images from 59 subjects ranged from 0- to 21-year old to quantify the shape and size change of the pediatric brain due to growth. Thus far, this is the only study focusing on developing a 3D statistical geometry model related to pediatric head. However, the global stiffness of a pediatric head is dominated by the skull and suture, therefore, to accurately assess pediatric head injuries,

**FIGURE 12. Test and simulation comparison in compression condition.²⁰**

detailed skull and suture geometry are necessary. In this study, a statistical head geometry model including head size, shape, suture size, and skull/suture thickness was developed based on CT images from 11 subjects, which is the first time that 3D geometry of pediatric skull and suture was quantified in a detailed manner.

Using mesh morphing method to rapidly develop FE models with different geometries has been reported before in the literature,⁴ but has never been applied to develop pediatric head FE models, in which accurately

modeling suture size and skull thickness are crucial. In this study, RBF was utilized to morph a 6-month-old child head FE model into three different pediatric head geometries with different skull/suture thickness distributions based on the statistical child head geometry model. Because the heads from 0- to 6-month-old infants are morphologically similar, the RBF method is very robust for morphing the baseline model into different geometries in the current study, which is proved by the high mesh qualities sustained by the morphed models. Moreover, because the landmarks were selected not only throughout the skull, but also along the skull-suture borders, the morphed model could accurately represent suture size and skull/suture thickness distribution.

The method of developing a parametric pediatric head FE model used in this study can be widely used for future investigations on pediatric head response and injury tolerance. This study demonstrated the feasibility of using a parametric pediatric head FE model to account not only material effects but also effects of changes in head geometry due to child growth, which is a significant improvement from previous pediatric head impact simulations.

Parametric Study on Material Properties and Morphology of Pediatric Head

The results of the parametric study on material properties of pediatric head indicate that the material properties of brain (G_0 , G_∞ , and β) had little influence on head peak acceleration, maximal principal stress, and strain of skull, which is consistent with the findings reported by Roth *et al.*²⁸ In another study conducted by Coats *et al.*,⁹ the material property of the pediatric brain was modeled as a visco-hyper-elastic material, and it was found that decreasing the brain ground-state shear modulus 50% did not significantly affect the skull stress response, but a much stiffer brain (about four times of the baseline) would increase the peak principal stress in the skull by 38% and increased peak force by 27%. One possible reason for this discrepancy could be that the test condition used in Coats' study was more severe (dropping from 0.82 onto stone) than those in the current study and thus resulted in increased brain deformation.

The morphology (size and geometry) of a child head vary significantly in the first 3 years of life. In this study, because subject's ages were within 0–3 months, the effects of head morphologic changes on the head response measurements were also limited. However, head geometry was significant in determining maximal stress in the skull and maximal strain in the suture after controlling skull material, indicating that head geometry plays an important role in determining the

pediatric head impact response. It is also reasonable to believe that the effect on head response from head morphological changes due to age will be much greater, if larger age range is considered.

Material Parameter Optimization and Model Validation

As mentioned earlier, there is large variation in pediatric head material properties in the literature. To determine the material parameters for different head components, an optimization method was used by matching the calculated head responses to the test results reported by Prange *et al.*,²⁰ which is the only study using the cadaver tests to quantify head responses during impact conditions. However, Prange *et al.* only tested three newborn infant heads at the age of 1-, 3-, and 11-day old. The peak head acceleration from the 1-day-old subject is substantially higher than the other two, which increased the average acceleration as well as its standard deviation. The same specimen also had significantly lower mass than the other two. In this study, the geometry of head FE model is based on statistical analysis of head landmarks describing the head geometry of 11 subjects, and its mass is close to the two test specimens with greater masses in the Prange *et al.*²⁰ study. Therefore, it is reasonable that optimization results might overestimate the stiffness of the 1-day-old head. More pediatric cadaver tests are necessary to further validate the parametric child head model developed in this study.

Limitations and Future Works

The most important limitations of this study are the small number of subjects (11) used to create the model of skull and suture geometry, and the small amount of pediatric cadaver data available with which to tune and validate the model performance. The sex and race of the subjects were not considered either because of the small sample size. Analysis of CT data from more subjects is needed to develop a more accurate pediatric head geometry model that better quantifies both the average developmental changes in head geometry and the variance within age. Nevertheless, the current study set up the framework for future applications, and can be considered as a good first step to develop a highly accurate pediatric head model.

Because the parametric model developed in this study can only represent heads from 0- to 3-month-old children, the material properties were assumed to be the same at different ages. Further investigation is needed to develop a relationship between age and material properties for different head components.²¹ In addition, anatomical regions among the brain, such as the cerebrum, cerebellum, and brain stem, cannot be

clearly differentiated due to the limited resolution of CT images. Future studies using MRI data are needed to develop a more detailed statistical brain geometry model for children and to investigate the pediatric brain injury.

CONCLUSIONS


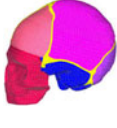


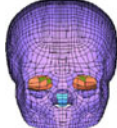
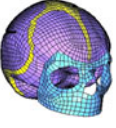
A PCA and regression approach was used to produce a statistical cranium geometry model based on head CT images from 11 children aged 0–3 months. An automatic mesh morphing method based on RBF was used to morph a baseline head FE model into three models representing newborn, 1.5-month-old, and 3-month-old infant heads. A parametric study was conducted using these three models to investigate the effects from material parameters and head geometries on the head responses during drop conditions. Results showed that the elastic modulus of skull had the most important effect on most head response measurements.

The head geometry also affected the maximal principal stress of the skull and the maximal principal strain of the suture after controlling the skull material. Material parameters of the brain had little effects on the head responses. Compared with the newborn child head, the 3-month-old head predicted higher peak head acceleration, and stress and strain in the suture, but lower stress and strain in the skull. Material properties of the head can be well determined by optimization method, and elastic moduli of skull, suture, dura, and scalp were 171, 8.0, 21, and 8.6 MPa, respectively, after optimization. The finding of this study indicated that it is important to consider the material properties and geometric variations together when estimating pediatric head responses and predicting head injury risks.

APPENDIX

See Table A1.

TABLE A1. Child head global FE models.

First author/ year	Lapeer/2001	Klinich/2002	Coats/2007	Roth/2007 and 2008	Roth/2007 and 2009	Roth/2010
Software	ABAQUS	LSDYNA	ABAQUS	RADIOSS	RADIOSS	RADIOSS
Figure						
Age	Fetal (new born)	6 months	1.5 months	6 months	3-year old	17-day old
Source of geometry	Multi-viewed laser scanning	CT	CT and atlas	CT	CT	CT
Components	Cranial bones Fontanels and sutures Skull base Maxilla	Cranial bones Skull base Fontanels and sutures Dura CSF brain Scalp face	Skull Brain Suture Scalp	Skull sutures Flax brain CSF scalp Face	Skull sutures Face CSF Falx brain Scalp	Skull Membranes Sutures CSF Brain scalp
Elements	63,413 shell elements	38,454 elements	32,881 elements	78,511 elements	26,500 elements	33,700 elements
Validation	Skull deformation data ³⁰ –		Cadaver test ^{35,36}	–	–	Cadaver test ²⁰
Applications	Fetal skull deformation subjected to uterine pressures; Fetal head subjected amniotic and cervical pressures	Three motor-vehicle accident reconstructions	Parametric study on brain material properties and suture geometry	Accident reconstructions for baby shaking	25 fall accident reconstructions	Accident reconstruction

ACKNOWLEDGMENTS

This project is funded by University of Michigan Transportation Research Institute, State Key Laboratory of Automotive Safety and Energy from Tsinghua University and China Scholarship Council Postgraduate Scholarship Program. The authors would like to thank Dr. Zhendan Xue in ESTECO for modeFRONTIER technical support.

CONFLICT OF INTEREST

There are no conflicts of interest in the work related to this manuscript.

REFERENCES

- ¹Atabaki, S. M. Pediatric head injury. *Pediatr. Rev.* 28(6):215–224, 2007.
- ²Ballesteros, M. F., R. A. Schieber, et al. Differential ranking of causes of fatal versus non-fatal injuries among U.S. children. *Inj. Prev.* 9(2):173–176, 2003.
- ³Bennink, H. E., J. M. Korbeeck, B. J. Janssen, et al. Warping a Neuro-Anatomy Atlas on 3D MRI Data with Radial Basis Function. In: International Federation for Medical and Biological Engineering Proceedings, Vol. 15, 2007, pp. 28–32.
- ⁴Besnault, B., F. Lavaste, H. Guillemot, et al. A Parametric Finite Element Model of the Human Pelvis. In: Proceedings of 42nd Stapp Car Crash, Paper No. 983147, 1998, pp. 1–15.
- ⁵Blanz, V., and T. Vetter. A Morphable Model for the Synthesis of 3D Faces. In: Proceedings of the 26th Annual Conference on Computer Graphics and Interactive Techniques, 1999, pp. 187–194.
- ⁶Carr, J. C., R. K. Beatson, J. B. Cherrie, et al. Reconstruction and Representation of 3D Objects with Radial Basis Functions. In: Proceedings of the 28th Annual Conference on Computer Graphics and Interactive Techniques, 2001, pp. 67–76.
- ⁷CDC. Childhood injuries in the United States. *Am. J. Dis. Child.* 144:627–646, 1990.
- ⁸Coats, B., and S. S. Margulies. Material properties of human infant skull and suture at high rates. *J. Neurotrauma* 23(8):1222–1232, 2006.
- ⁹Coats, B., S. S. Margulies, and S. Ji. Parametric study of head impact in the infant. *Stapp Car Crash J.* 51:1–15, 2007.
- ¹⁰Danelson, K. A., C. P. Geer, et al. Age and gender based biomechanical shape and size analysis of the pediatric brain. *Stapp Car Crash J.* 52:59–81, 2008.
- ¹¹Dekaban, A. S. Tables of cranial and orbital measurements, cranial volume, and derived indexes in males and females from 7 days to 20 years of age. *Ann. Neurol.* 2(6):485–491, 1977.
- ¹²Franklyn, M., S. Peiris, C. Huber, and K. H. Yang. Pediatric material properties: a review of human child and animal surrogates. *Crit. Rev. Biomed. Eng.* 35(3–4):197–342, 2007.
- ¹³Jonathan, C. C., W. R. Fright, and R. K. Beatson. Surface interpolation with radial basis function for medical image. *IEEE Trans. Med. Imag.* 16:96–107, 1997.
- ¹⁴Klinich, K. D., G. M. Hulbert, and L. W. Schneider. Estimating infant head injury criteria and impact response using crash reconstruction and finite element modeling. *Stapp Car Crash J.* 46:165–194, 2002.
- ¹⁵Kraus, J. F., A. Rock, and P. Hemyari. Brain injuries among infants, children, adolescents, and young adults. *Am. J. Dis. Child.* 144:684–691, 1990.
- ¹⁶Langlois, J. A., W. Rutland-Brown, and K. E. Thomas. Traumatic brain injury in the united states: emergency department visits, hospitalizations, and deaths. Atlanta, GA: Centers for Disease Control and Prevention, National Center for Injury Prevention and Control, 2006.
- ¹⁷Lapeer, R. J., and R. W. Prager. Fetal head moulding: finite element analysis of a fetal skull subjected to uterine pressures during the first stage of labour. *J. Biomech.* 34(9):1125–1133, 2001.
- ¹⁸Nelder, J. A., and R. Mead. A simplex method for function minimization. *Comput. J.* 7(4):308–313, 1965.
- ¹⁹Park, J., and J. W. Sandberg. Universal approximation using radial basis functions network. *Neural. Comput.* 3:246–257, 1991.
- ²⁰Prange, M. T., J. F. Luck, A. Dibb, et al. Mechanical properties and anthropometry of the human infant head. *Stapp Car Crash J.* 48:279–299, 2004.
- ²¹Prange, M. T., and S. S. Margulies. Regional, directional, and age-dependent properties of the brain undergoing large deformation. *J. Biomech. Eng.* 124:244–252, 2002.
- ²²Reed, M. P., and M. B. Parkinson. Modeling Variability in Torso Shape for Chair and Seat Design. In: Proceedings of the ASME Design Engineering Technical Conferences, Paper No. 2008-49483, 2008, pp. 1–9.
- ²³Reed, M. P., M. M. Sochor, J. D. Rupp, K. D. Klinich, and M. A. Manary. Anthropometric specification of child crash dummy pelvis through statistical analysis of skeletal geometry. *J. Biomech.* 42(8):1143–1145, 2009.
- ²⁴Roche, A. F. Increase in cranial thickness during growth. *Hum. Biol.* 25(2):81–92, 1953.
- ²⁵Roth, S., J. S. Raul, B. Ludes, and R. Willinger. Finite element analysis of impact and shaking inflicted to a child. *Int. J. Legal Med.* 121(3):223–228, 2007.
- ²⁶Roth, S., J. S. Raul, J. Ruan, and R. Willinger. Limitation of scaling methods in child head finite element modelling. *Int. J. Veh. Saf.* 2(4):404–421, 2007.
- ²⁷Roth, S., J. S. Raul, and R. Willinger. Biofidelic child head FE model to simulate real world trauma. *Comput. Methods Programs Biomed.* 90:262–274, 2008.
- ²⁸Roth, S., J. S. Raul, and R. Willinger. Finite element modelling of paediatric head impact: global validation against experimental data. *Comput. Methods Programs Biomed.* 99:25–33, 2010.
- ²⁹Roth, S., J. Vappou, J. S. Raul, and R. Willinger. Child head injury criteria investigation through numerical simulation of real world trauma. *Comput. Methods Programs Biomed.* 93(1):32–45, 2009.
- ³⁰Sorbe, B., and S. Dahlgren. Some important factors in the molding of the fetal head during vaginal delivery—a photographic study. *Int. J. Gynaecol. Obstet.* 21(3):205–212, 1983.
- ³¹Synder, R. G., L. W. Schneider, et al. Anthropometry of Infants, Children, and Youths to Age 18 for Product Safety Design. Bethesda, MD: U.S. Consumer Product Safety Commission, 1977.
- ³²Thibault, K. L., and S. S. Margulies. Age-dependent material properties of the porcine cerebrum: effect on pediatric inertial head injury criteria. *J. Biomech.* 31:1119–1126, 1998.

- ³³Turk, M., and A. Pentland. Eigenfaces for recognition. *J. Cogn. Neurosci.* 3(1):71–86, 1991.
- ³⁴Viano, D., H. von Holst, and E. Gordon. Serious brain injury from traffic related causes: priorities for primary prevention. *Accid. Anal. Prev.* 29(6):811–816, 1997.
- ³⁵Weber, W. Experimental studies of skull fracture in infant. *Z. Rechtsmed.* 92(2):87–94, 1984.
- ³⁶Weber, W. Biomechanical fragility of the infant skull. *Z. Rechtsmed.* 94(2):93–101, 1985.
- ³⁷Willinger, R., and L. Taleb. Modal temporal analysis of head mathematical models. *J. Neurotrauma* 12(4):743–754, 1995.
- ³⁸Zhang, L., K. H. Yang, and A. I. King. Comparison of brain responses between frontal and lateral impacts by finite element modeling. *J. Neurotrauma* 18(1):21–30, 2001.